

Comparison of two ceiling-based ventilation strategies for twin-aisle aircraft cabins

Pascal Lange^{1,*}, Tobias Dehne¹, Daniel Schmeling¹, Axel Dannhauer¹, Ingo Gores²

¹ German Aerospace Center (DLR), Institute of Aerodynamics and Flow Technology, Bunsenstr. 10, 37073 Göttingen, Germany

² Airbus Operations GmbH, Kreetzlag 10, 21129 Hamburg, Germany

*Corresponding email: pascal.lange@dlr.de (Pascal Lange)

SUMMARY

Two novel, ceiling-based ventilation techniques for aircraft, comprising micro-jet ventilation and low-momentum-ceiling-ventilation are analyzed experimentally under two different thermodynamic boundary conditions representing different operational flight phases. By means of a measurement system based on local probes, the two systems are compared to each other addressing the topics of thermal passenger comfort and energy efficiency. Thus, the studies are directly in-lined with the goals of the EU to reduce the carbon dioxide emission caused by aviation. Regarding the temperature homogeneity, temperature stratifications near the passengers, fluid velocities as well as heat removal efficiency, both concepts performs similar characterized by overall thermally comfortable conditions. However, differences occurred by comparing the systems under different thermodynamic boundary conditions. For both systems, the thermal passenger comfort and energy efficiency rating is significantly increased under warmer ambient conditions.

KEYWORDS

Aircraft cabin, crown-integrated ventilation, thermal passenger comfort, energy efficiency

1 INTRODUCTION

Passenger compartments of commercial aircraft are one of the most complex indoor environments in mass public transport sector (Elmaghraby et al. 2018). Accordingly, novel ventilation concepts for aircraft cabins have attracted the attention of scientists and manufactures for decades due to their potential of energy and weight-saving along with the optimization of thermal passenger comfort and air quality management. In addition to that, alternative ventilation strategies are promising to reconsider the cabin layout in terms of industrial modularization of the cabin to improve manufacturing processes economically. Here, the simplification of customizing aircraft cabin's design and architecture is of high interest for manufactures (A³, 2018). These are just a few facts justifying the need of novel ventilation strategies for modern passenger aircraft. In previous studies, cabin displacement ventilation (CDV) as an alternative ventilation approach was analyzed in twin-aisle as well as single-aisle cabin geometries (Zhang and Chen, 2007; Bosbach et al. 2012). Since different thermodynamic boundary condition occur during a flight – dependent on the different flight phases – the latter work even considers realistic stationary and non-stationary boundary conditions by conducting flight tests in an A320 of the German Aerospace Center (DLR). Nevertheless, besides the benefits of pure CDV some drawbacks regarding comfort critical temperature stratifications were observed. To avoid costly and time-intensive flight tests, the presented experimental studies are conducted in the new modular cabin mock-up (MKG) of the DLR.

The aim of the present work is the experimental investigation of two crown-integrated ventilation scenarios for twin-aisle layouts. Here, both concepts are analyzed under realistic thermodynamic boundary conditions to evaluate similarities and differences between both systems in terms of thermal passenger comfort and energy efficiency.

2 EXPERIMENTAL SET-UP

Figure 1a) shows the MKG, a test facility for aircraft cabin research activities. It represents a wide-body aircraft cabin section on a scale of 1:1. The mock-up is equipped with realistic interior parts such as linings, overhead bins and seats. During the measurements, thermal manikins (TMs) are installed on all seats, where each of them can be heated individually to simulate the sensible heat release of passengers. The installed seating layout is based on a 10-abreast seating configuration with a 3-4-3 seat arrangement, see Figure 1b). In total, 10 seat rows are installed in the MKG, resulting in a seating capacity of 100. The total inner volume of the MKG amounts to 126.5 m³.

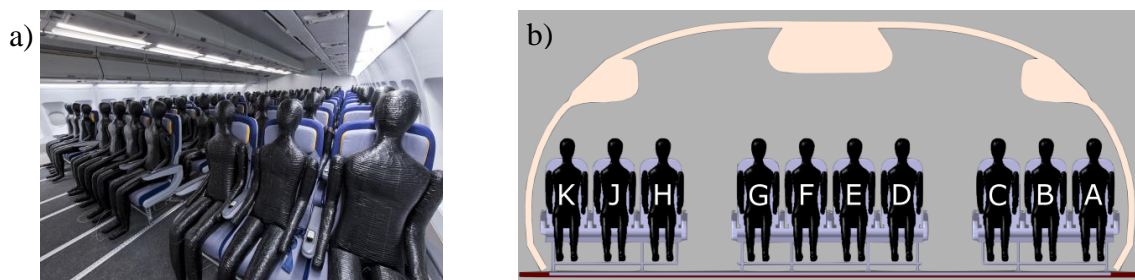


Figure 1. Test environment MKG. a) Inner view with TMs. b) Sketch of seating layout including labels.

Since realistic boundary conditions – both geometrically and thermodynamically – are crucial for the evaluation of novel ventilation strategies, the facility enables the simulation of thermodynamic realistic boundary conditions. By means of temperature-controlled fuselage elements, the gap temperature (T_{gap}) between primary and secondary insulation layer can be simulated experimentally, which differs depending on the operational phases. During these studies, two different flight scenarios are considered: normal flight conditions for cruising and a Hot-Day-on-Ground (HDoG) case representing the departure of an airliner at very warm ambient temperatures.

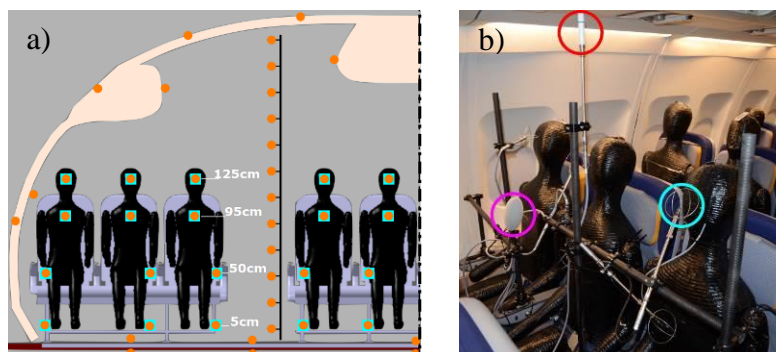


Figure 2. Sensor installation. a) Positions of RTDs (orange circles) and OVPs (cyan squares) within the MKG. b) Comfort sense system based on OVP (cyan circle), humidity (red circle) and operative temperature probe (magenta circle).

A comprehensive measurement system is installed to determine comfort-relevant quantities and ventilation efficiency parameters. During the tests, each TM is operated in an

automatically-controlled mode for the heat release. The underlying control algorithm is based on the human heat release – cabin temperature curve according to (EN13129, 2016) and represent a value of 82 W (for each TM) for the considered mean cabin temperature (T_{cab}). To determine the temperature homogeneity in the entire cabin, resistance temperature detectors (RTDs) are installed at chest height in front of all TMs. Moreover, as shown in Figure 2a), 10 measurement racks equipped with RTDs at four height levels (ankle, knee, chest and head) are mounted close to the TMs to acquire temperature stratifications near the manikins and to determine T_{cab} as an average over these 40 RTDs in row 4. An additional rack with 12 RTDs at different height is placed in the aisle, close to seat row 5. Further sensors are installed at the inner surfaces, outside the cabin and also behind the linings, see Figure 2a). The latter are used to monitor the values of the temperature-controlled fuselage elements. In total, more than 250 RTDs are installed, where each provide an accuracy of better than ± 0.15 °C. Omnidirectional velocity probes (OVPs) are used to measure the fluid velocities near the TMs. Here, 10 racks are installed at row 6 similarly to the positioning of the RTDs, see Figure 2a). Those sensors enable the measurement of velocities and temperatures simultaneously. Herewith, draft risk is detectable and further the knowledge of the flow velocities is important to determine large-scale flow patterns as well as small-scale turbulence structures which affect the mixing behavior and the heat exchange within the cabin. The OVPs provide an accuracy of 0.02 m/s for velocity and 0.2 K for temperature measurements. As indicated in Figure 2b), the system is enhanced by comfort sense probes to acquire climate indices, such as Predicted Mean Vote (PMV) and Predicted Percentage of Dissatisfied (PPD), which combine several comfort-relevant flow quantities. However, in the current configuration, the comfort sense system is only installed at two specific seats (6J and 6K).

2 STUDIED CONCEPTS

With respect to increase the degree of prefabrication for optimized aircraft manufacturing, the novel ventilation concepts are fully integrable in the crown of an aircraft. Hence, the two studied concepts introduced in this work are ceiling-based ventilation systems. The first analyzed concept is a generic version of a micro-jet ventilation (MJV), which is well-known and state-of-the-art for air conditioning of long-distance trains. As indicated in Figure 3a), inclined and straight aligned air inlets are installed in the whole ceiling area of the MKG. These inlets are based on perforated ceilings, whereby the fresh air is supplied as localized micro-jets with a rather high momentum of approximately 0.5 m/s. After circulation, the air leaves the compartment through openings located on both sides on floor level.

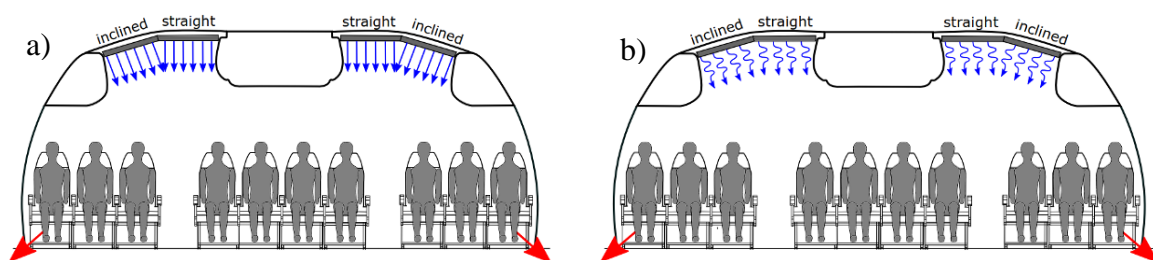


Figure 3. Studied ventilation approaches. a) Illustration of MJV. b) Illustration of LMCV.

The second concept is the low-momentum-ceiling-ventilation (LMCV). It is characterized by a low-momentum air supply through planar and large-surface inlets, which are similarly aligned in the ceiling area as described for MJV, see Figure 3b). The inlet area is made of fabric membranes, which ensures a uniform outflow with flow velocities of less than 0.05 m/s. The exhaust openings are also located at floor level.

All studied cases with the corresponding boundary conditions, such as flow rate (V), gap temperature (T_{gap}) as well as temperature for supplied (T_{in}) and exhausted air (T_{out}) are summarized in Table 1. As a note, T_{cab} serves as a control temperature and is kept constant with a maximum deviation of 0.1 K during the state of equilibrium. To reach the setpoint of $T_{\text{cab}} = 23 \text{ }^\circ\text{C}$ and keep it constant, T_{in} is adjusted individually for each studied case.

Table 1. Investigated test scenarios including corresponding boundary conditions.

Scenario no.	Ventilation	Flight phase	V [m^3/s]	T_{gap} [$^\circ\text{C}$]	T_{in} [$^\circ\text{C}$]	T_{out} [$^\circ\text{C}$]
#1	MJV	Cruise	1	10.5	18.0	20.3
#2	LMCV	Cruise	1	10.1	18.0	21.0
#3	MJV	HDoG	1	35.1	16.3	22.5
#4	LMCV	HDoG	1	35.0	14.2	22.7

3 RESULTS AND DISCUSSION

First thing to note is, that the presented results of the fluid temperatures and velocities are based on time-averaged data (1800s during the state of equilibrium). In a second step, the data is evaluated and prepared as shown in the upcoming subsections.

Fluid temperatures

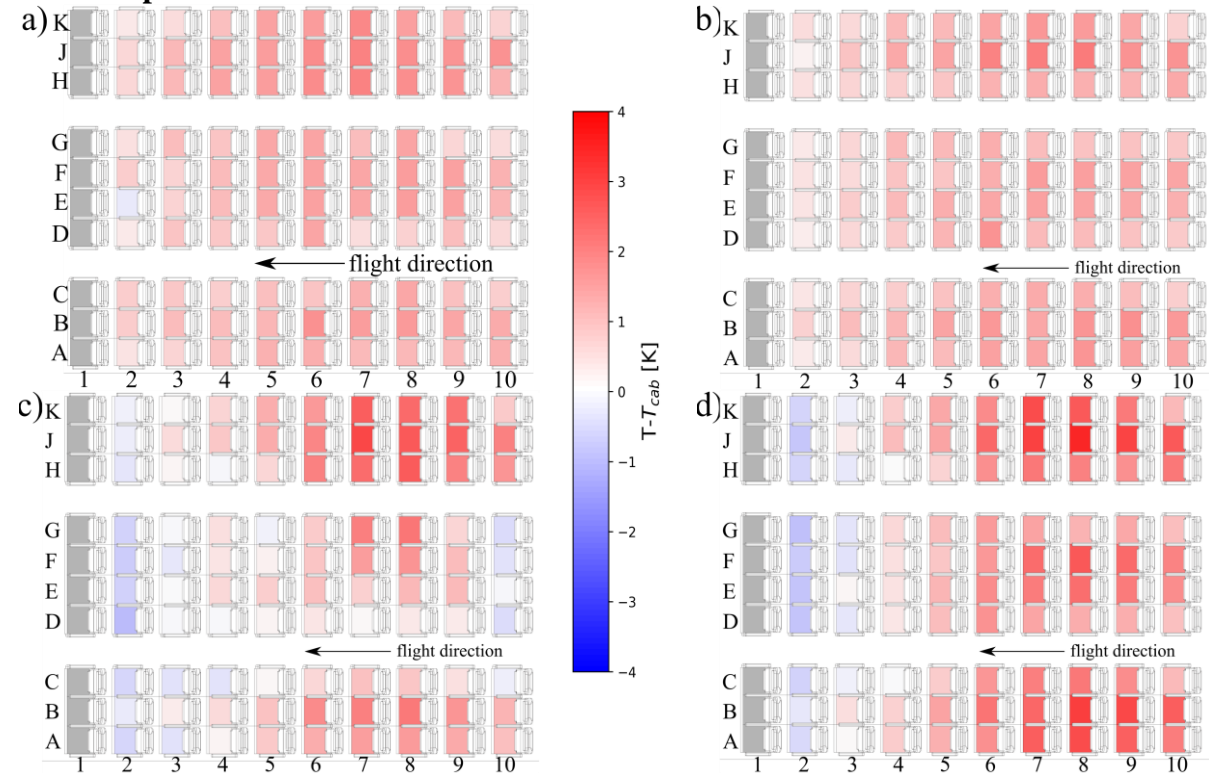


Figure 4. Fluid temperatures near the TMs at chest level. The data is given as difference to the mean cabin temperature. a) Scenario #1. b) Scenario #2. c) Scenario #3. d) Scenario #4.

Figure 4 depicts the chest temperatures in vicinity of the TMs for the scenarios #1 to #4 as contour plots in top view to analyze the temperature homogeneity within the cabin. For the sake of comparability, the temperature data is given as differences to the respective mean cabin temperature (T_{cab}). First thing to note for all cases is, that significant lower temperatures of up to -3 K compared to the mean cabin temperature occurred in the first row. These inhomogeneities are caused by boundary effects due to missing heat loads in front of the first row. Hence, the specific seat row is greyed out and is not considered for the interpretation of the results. Generally, both studied ventilation systems provide a more homogeneous

temperature distribution under cruise conditions, see Figure 4a) and b), compared to HDoG conditions. At scenario #1 and #2, the temperature homogeneity is characterized by deviations of +1.3 K relative to T_{cab} for 90% of the seats. For both cases, a maximum deviation of +2 K is determined at a single seat position (7J). In contrast, under HDoG conditions (see scenario #3 and #4) the temperature distribution reveals inhomogeneities for both systems characterized by standard deviations (calculated for the 90 considered values) twice as large compared to case #1 and #2. At #3 maximum values of +2.9K occurred, whereas at #4 the maximum deviation amounts to +3.4K. Due to the warm floor and the cold ceiling area under HDoG conditions, it seems that a large-scale flow structure in longitudinal direction is developed comparable to a Rayleigh-Bérnard convection. The warmer fluid rises in the rear end of the cabin and descends in the first 3 seat rows after passing the cooler ceiling, where the fresh air is supplied. This could cause the colder seat position in the first three seat rows with values of up to -2.8 K relative to T_{cab} and the warmer fluid temperatures in the rear row of seats. However, this theory needs to be verified in upcoming measurement campaigns.

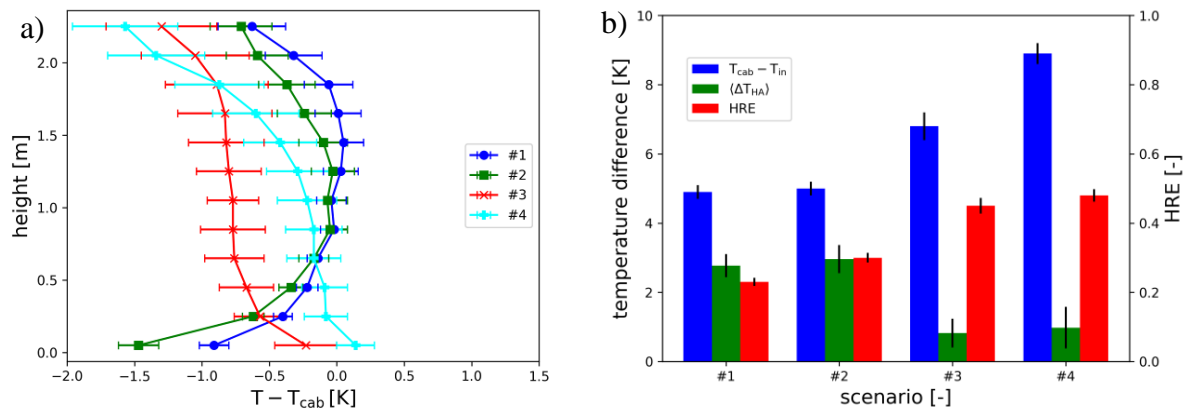


Figure 5. a) Time-averaged temperature stratification in the aisle. Values are given relative to the mean cabin temperature. b) Mean cabin temperature relative to inflow temperature, mean temperature difference between head and ankle level and heat removal efficiency.

The temperature stratifications and fluctuations in the aisle are addressed in Figure 5a). For the first two thirds of the cabin height (< 1.6 m), a significant temperature gradient of 1.0 K and 1.4 K is determined at #1 and #2, respectively. Here, the cooled surfaces, particularly the floor, lead to the lower temperatures at the bottom. Above the heating loads, i.e. above passengers' head level to the ceiling (> 1.6 m), the temperatures decrease again due to the cold incoming air. For the cruise case, both systems of MJV and LMCV provide a similar temperature profile, with values less than zero in the upper and lower third of the cabin and values close to zero in between. At #3 and #4, the values are close to zero right above the floor and decrease as the cabin height increases. Thus, the effect of the changing thermodynamic boundary conditions and flow structures of the studied scenarios is directly affecting the vertical temperature distribution in the cabin. The error bars in Figure 5a) depict the temporal standard deviation, which are reflecting the strength of the velocity fluctuations. For all scenarios (#1 to #4), a region of pronounced temperature fluctuations is determined above a height of 1.75 m increasing the threshold of 1.5 time the value at floor level. These are the result of the air supply at ceiling level, leading to major variations of the fluid temperatures in the aisle. Under HDoG conditions, the vertical temperature distributions of both systems (#3 and #4) are significantly different compared to cruising. Here, a monotonic temperature drop is determined from the floor to the ceiling, resulting in an unstable thermal stratification with the highest temperatures on floor level. While at #3, the temperature decreases by 1.1 K, the drop is more pronounced with 1.7 K at #4. In general, MJV provide a

lower temperature stratification in the aisle, however, changing thermodynamic boundary conditions strongly affect the results. Figure 5b) summarizes several findings based on fluid temperature measurements. At first, the temperature difference between T_{cab} and T_{in} is plotted for the studied scenarios, reflecting the required inflow temperature to reach a comfortable and constant cabin temperature. While under cruise conditions (#1 and #2), both systems perform equally with a difference of 5 K, the values rise via 7 K to 9 K for #3 and #4, respectively. That means, during a HDoG scenario LMCV (#4) required a lower inflow temperature level in contrast to MJV (#3) which provides the potential for energy savings in the ECS.

A further crucial quantity regarding passenger comfort, shown in Figure 5b) is the spatially averaged temperature difference between head and foot level (ΔT_{HA}). For all scenarios the value is in a comfortable range well below 3 K. Nevertheless, the data reveal the influence of the thermodynamic boundary conditions. The values at #1 and #2 are greater by a factor of 3 compared to #3 and #4. The comparison of MJV and LMCV shows only minor deviations. The last depicted quantity is the heat removal efficiency (HRE) as defined in Bosbach (2012). The HRE is a measure of how effectively heat is dissipated from the cabin by the ventilation system. According to the definition of this quantity, high HRE results in a reduced cooling demand for the incoming air and is thus desirable. It is noticeable, that the values are significantly lower for cruise conditions compared to the HDoG scenarios. At #1 and #2 the values amount to 0.23 and 0.30, respectively. The rather small HRE for both cases is due to the fact that a major part – more than 50% - of the released heat is dissipated via the fuselage elements. Under cruise conditions, this effect is supported by the large temperature gradient of roughly 4.5 K between the cabin air and the inner surfaces, as well as by the large areas of the adjoining cooled lining elements. For scenario #3 and #4, the HRE increases to 0.45 and 0.48, respectively. Here, the heat loss through the sidewalls do not exist since T_{gap} is higher than T_{cab} . Consequently, the warmed fuselage elements serve as an additional heat load so that a larger amount of heat is removed by the ventilation system. Generally, a comparison between both ventilation concepts reveals, that LMCV performs slightly better than MJV in terms of an effective heat removal.

Fluid velocities

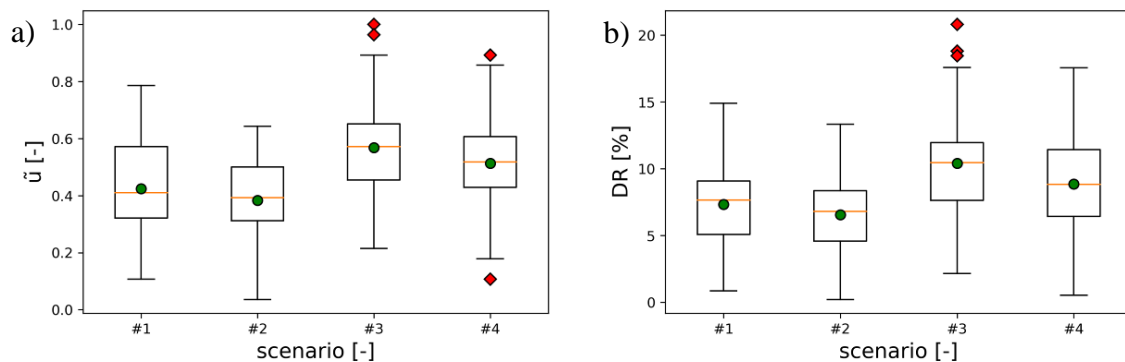


Figure 6. Box plots of the fluid velocities and the draft rates within the cabin. The median is marked as orange lines, the mean value as green dots and the outliers as red diamonds. a) Normalized velocity magnitudes near the TMs. b) Draft rate measured near the TMs.

The spatially averaged results of the measured fluid velocities near the TMs are summarized in Figure 6a) as boxplots for all studied scenarios. For the sake of comparability, the data is normalized with the global maximum measured for all cases. Clearly, the velocities are higher for the MJV concept (#1 and #3) in contrast to the LMCV scenario (#2 and #4) whether under cold or warm conditions. This indicates the higher momentum of the incoming air at MJV.

Comparing the two studied boundary conditions, the values at the cruise scenarios are lower than under HDoG conditions. During the latter, the temperature gradient between the incoming air and the surface of the TMs is greater than under cruise condition. As a result, the flow in the vicinity of the TMs is dominated by thermal convection, which might lead to slightly higher fluid velocities near the manikins. Regarding the mean velocities, #3 reveals a value of 0.6 of the maxima and thus the highest mean value of all configurations. The median of all scenarios covers a range from 0.4 to 0.6 of the maxima. To quantify the achievable passenger comfort, the draft rate (DR) is calculated based on the local temperature, velocity and turbulence level. DR describes the percentage of people bothered by draft. As an overview of the measured data, Figure 6b) shows the spatially averaged results of the DR near the TMs as boxplots for the studied scenarios. Generally, the DR under cruise conditions is lower compared to the HDoG cases. A more detailed analysis of the data reveals that under cruise conditions (case #1 and #2) the DR stays well below 15% for all measurement positions at seat row 6. However, values of slightly more than 10% DR are determined at some seats. For case #1, DR larger than 10% occurred at seat 6D, 6E, 6G, 6H, 6J and 6K. At case #2 only seat positions 6H, 6J and 6K are characterized by values greater than 10%. In contrast to cruise conditions, all positions except seat B reveal values greater than 10% for the HDoG cases (#3 and #4). Even DR over 15% occurred at seat 6D, 6G, 6H, 6J and 6K for case #3. At case #4 three seat positions (6H, 6J, 6K) are determined by a DR > 15%.

Comfort quantity of PMV and PPD

An additional rating of the thermal comfort is determined by means of PMV and PPD index for chest height (0.95 m above the floor) at two seat positions (seat 6J and 6K). Whereas the PMV values are measured using the comfort sense system described in section 2, PPD values are calculated according to (ISO 7730, 2005). The PMV index rates the comfort from cold via neutral to warm by means of a 7-point scale ranging from -3 to +3. PPD, however, presents a quantity of the percentage of thermally dissatisfied passengers feeling too cool or too warm. The data for the selected seat for the studied cases is summarized in Table 2.

Table 2. Averaged PMV and PPD values at seat 6J and 6K of the studied cases.

Index / scenario	#1	#2	#3	#4
PMV [-]	-0.8 ± 0.1	-0.8 ± 0.1	-0.5 ± 0.1	-0.6 ± 0.1
PPD [%]	17.5 ± 3.0	19.9 ± 2.8	9.9 ± 0.8	12.5 ± 1.3

Based on the PMV values, all investigated scenarios are rated as thermally comfortable according to ISO 7730 (2005). The comparison between the two studied ventilation approaches (#1 - #2 and #3 - #4) shows no significant differences. The PMV as well as PPD are equal within the limits of the measurement accuracy. However, the influence of the changed thermodynamic boundary conditions can be detected. At #1 and #2 the PMV values are -0.8, which still represents a neutral comfort rating, but tend to slightly to cold rating. The corresponding PPD reveal, that roughly 20% of the passengers are thermally dissatisfied with the climate provided by both ventilation systems under cruise conditions. In contrast, the two cases under HDoG conditions (#3 and #4) provide environmental conditions rated significantly better than under cruise conditions. Here, the higher temperatures at the fuselage elements affect the measured PMV values, resulting in a mean PMV index of roughly -0.6. The corresponding PPD values at #3 and #4 amount to 9.9% and 12.5%, respectively. According to the rating criteria given in ISO 7730 (2005), both cases are evaluated with a neutral thermal sensation. Here, just over 12% of the passengers feel uncomfortable by the thermal environment.

4 CONCLUSIONS

In the present work, the performance of two novel ventilation approaches for modern long-range airliners are experimentally analyzed and compared to each other in terms of passenger comfort and energy efficiency under two different thermodynamic boundary conditions. Both, micro-jet ventilation and low-momentum-ceiling-ventilation are fully integrable in the ceiling of an aircraft, which is beneficiary for the cabin design providing the potential for high prefabrication depth. The tests are conducted in the DLR's full-scale cabin mock-up, facilitating studies under different thermodynamic boundary conditions in order to simulate different operational flight phases. In this study, a cruise and a Hot-Day-on-Ground scenario are investigated. Generally, the comparison between the two air supply techniques of MJV and LMCV reveal many similarities under same thermodynamic boundary conditions by providing comfortable thermal conditions. The temperature homogeneity is comparable for both systems. Under cruise conditions, the deviation is less than +2 K, while colder spots occurred in the first 2 seat rows at HDoG. However, differences regarding the fluid velocities and DR can be observed. Due to the high inflow momentum at MJV, the fluid velocities near the manikins are higher compared to LMCV. As a result, almost twice as many seats are determined with $DR > 10\%$ (at cruise) and $DR > 15\%$ (at HDoG) for MJV in contrast to LMCV. Further, the inlet temperature of both systems significantly differs under HDoG conditions by 2.1 K. Here, LMCV provides a comparable comfort level with a lower T_{in} . In terms of comfort indices (PMV and PPD), both systems perform equally, while more comfortable conditions are achieved for the HDoG scenario. Regarding the energy efficiency, LMCV and MJV reveal a rather low HRE of less than or equal to 0.3 at cruise case. At HDoG, the heat removal efficiency of both systems increases by more than 30%.

To conclude, under steady boundary conditions both ventilation approaches performs comparable with minor differences in terms of fluid velocities and draft rates. However, significant differences were found when comparing two boundary conditions. This highlights the necessity of considering different thermodynamic boundary conditions for evaluating the robustness of new ventilation concepts.

In upcoming studies, the evaluation methods will be extended by measurements addressing the air quality level by means of tracer gas measurements. Further, experiments under transient boundary conditions will be conducted.

ACKNOWLEDGEMENT

This project has received funding from the Clean Sky 2 Joint Undertaking under the European Union's Horizon 2020 research and innovation programme under grant agreement No. 755596.

6 REFERENCES

- Bosbach J, Heider A, Dehne T, Markwart M, Gores I, and Brendfeldt P. 2012. Evaluation of Cabin Displacement Ventilation under Flight Conditions. *28th International Congress of the Aeronautical Sciences ICAS*, Brisbane, Australia.
- Elmaghraby H.A, Chiang Y.W, and Aliabadi A.A. 2018. Ventilation strategies and air quality management in passenger aircraft cabins. *Sci. Technol. Built. Environ.*, Vol. 24, No. 2, pp 160-175.
- EN13129 - European Committee for Standardization. 2016. *EN 13129: Railways Application: Air Conditioning for Main Rolling Stock, Comfort Parameters and Type Tests*.
- ISO 7730 – International Standard Organization. 2005. *DIN EN ISO 7730: Ergonomics of the thermal environment*
- Zhang C. and Chen Q. 2007. Novel air distribution systems for commercial aircraft cabins. *Built. Environ.*, Vol. 42, No. 4, pp 1675-1684